Scientia Iranica, Vol. 15, No. 5, pp 644–651
© Sharif University of Technology, October 2008
SCIENTIA
IRANICA

Research Note

Some New Robust Pseudo Forward and Rotation Gaits for the Snakeboard

A. Asnafi[1] and M. Mahzoon[2,*]

The goal of this paper is to introduce some new robust gaits of the snakeboard. This is achieved by defining two parameters; the ratios of the frequencies and amplitudes of the snakeboard's sinusoidal shape variable dynamics, and properly adjusting their variations. The gaits are produced via stable and/or moving limit cycles. The highly symmetric patterns generated by these gaits, besides their inherent beauty and coherency, exemplify the rich information content of the underlying nonlinear system.

INTRODUCTION

The snakeboard is the modified model of a skateboard. It is composed of a rigid bar with two connected wheel-based platforms, which can pivot freely about the vertical axes (see Figure 1). The rider puts his/her feet on the platforms and generates motion by coupling the twisting of his/her torso with an appropriate turning of his/her feet on the platforms without touching the ground.

A simplified model of the snakeboard studied in the literature is illustrated in Figure 2.

This model was first studied by Lewis et al. [1] and its three famous gaits, i.e. forward, rotation and parallel parking, were developed. It has also been studied in the literature as the prototype of a robotic locomotion system, which is modeled via geometric tools (see, for example [2-4]). The controllability idea for the snakeboard was given first by Ostrawki and Burdick [5,6] and then followed by Bullo, Leonard, Lewis and Lynch [7,8]. The snakeboard also has been studied in the literature as a kinematically underactuated system. Ostrowski [9] derived an approximate path generation algorithm by using the studies of Murray and Sastry [10] on kinematic systems. He also described, numerically, an optimal trajectory generation [11] with the collaboration of Desai and Kumar. Some new research on the motion planning of the snakeboard that has an analytical approach and which is all based on kinematic reduction, was developed by Bullo and Lynch [12], Bullo and Lewis [13] and Iannitti and Lynch [14,15]. Recently, Shammas [16] has developed some general rules for gait generation in a snakeboard. He has considered three types of gait: Purely kinematic, purely dynamic and kino-dynamic. In almost all previous work on the subject, the nonlinear behavior of this dynamic system is not addressed.

In this paper, the focus is on the nonlinear behavior of the snakeboard as a nonlinear locomotive system and, through the suitable tuning of input parameters,

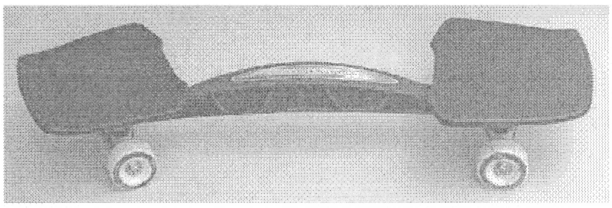

Figure 1. The snakeboard.

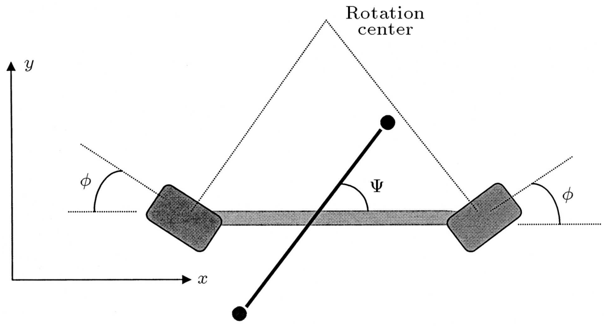

Figure 2. The simplified model of the snakeboard.

1. *Department of Mechanical Engineering, School of Engineering, Yasouj University, Yasouj, 75914, Iran.*
2. *Department of Mechanical Engineering, School of Engineering, Shiraz University, Shiraz, 7134813668, Iran.*
*. *To whom correspondence should be addressed. E-mail: mahzoon@shirazu.ac.ir*

some new robust gaits will be produced with stable and moving limit cycles. Because the snakeboard is usually considered as a prototype of a symmetrical nonholonomic locomotive system, these results may help to further elucidate some salient features of these nonlinear systems.

NONHOLONOMIC SYSTEMS WITH SYMMETRIES

In the literature, the snakeboard has been presented as an example of a robotic locomotion system that has both nonholonomic constraints and symmetries. In this paper, first, some basic ideas and concepts pertinent to these systems are reviewed, via a geometric approach (see, for example [17-19]).

Unconstrained Affine Connection Control System

Assume that the configuration space of the described system with coordinates $\{q^1, q^2, \cdots, q^n\}$ is Q, having defined on it the kinetic energy metric, $G(q)$, and also an inner product, $\langle\langle ., . \rangle\rangle$, acting between its vector fields. Define the affine connection, ∇, associated with $G(q)$ and Q, as a map, which assigns to vector fields X and Y the covariant derivative of Y, with respect to X denoted by $\nabla_X Y$ with coordinates:

$$(\nabla_X Y)^i = \frac{\partial Y^i}{\partial q^j} X^j + \Gamma^i_{jk} X^j Y^k, \tag{1}$$

where:

$$\Gamma^i_{jk} = \frac{1}{2} G^{li} \left(\frac{\partial G_{lk}}{\partial q^j} + \frac{\partial G_{lj}}{\partial q^k} - \frac{\partial G_{kj}}{\partial q^l} \right). \tag{2}$$

If m external forces, $F_1, F_2, \cdots, F_m$, which are described as m one-forms, are applied to the system, then, the equation of motion is [20]:

$$\ddot{q}^i + \Gamma^i_{jk} \dot{q}^j \dot{q}^k = \sum_{a=1}^{m} G^{il} (F_a)_l u_a, \tag{3}$$

where $(F_a)_l$ is the lth-component of F_a and u_a is the possible corresponding control.

The coordinate free form of the above equation is as follows:

$$\nabla_{\dot{q}} \dot{q} = \sum_{a=1}^{m} (G^{-1} F_a) u_a. \tag{4}$$

Affine Connection Control System with Nonholonomic Constraints and Symmetries

Assume that the non-integrable constraints of the system, i.e. nonholonomic constraints, are linear in $\dot{q}$. They can, thus, be written as follows:

$$\omega^i_j \dot{q}^j = 0, \qquad i = 1, \cdots, k, \tag{5}$$

where k is the number of constraints. Also, the coordinate free format of Equation 5 is:

$$\langle \omega, \dot{q} \rangle = 0,$$

when $\langle ., . \rangle$ is the natural pairing between tangent and cotangent vector fields on Q and ω is constrained one-forms $\{\omega_1, \omega_2, \cdots, \omega_k\}$.

The constraint distribution, D, is defined as the s dimensional distribution (i.e., the set of all velocities that satisfy the constraints) of feasible velocities, where $s = \dim(Q) - k = n - k$.

Let $P : TQ \to D$ be the orthogonal projection on D (orthogonality, of course, is defined with respect to G), $P^\perp = I - P$, where I is the identity tensor and, also, $D^\perp$ is the orthogonal complement of D with respect to G.

By using the above assumptions and definitions, the equation of motion for nonholonomic systems with symmetries can be written as [4]:

$$\nabla_{\dot{q}} \dot{q} = \lambda + \sum_{a=1}^{m} (G^{-1} F_a) u_a, \qquad P^\perp(\dot{q}) = 0, \tag{6}$$

where λ is the Lagrange multiplier vector which belongs to $D^\perp$.

Here, a lemma and a theorem developed in [20] are demonstrated, which transform Equations 6 into a format more suitable for application to these systems.

Lemma

Equations 6 can be written as:

$$\tilde{\nabla}_{\dot{q}} \dot{q} = \sum_{a=1}^{m} (P G^{-1} F_a) u_a, \tag{7}$$

where $\tilde{\nabla}$ is the affine connection given by:

$$\tilde{\nabla}_X Y = \nabla_X Y + (\nabla_X P^\perp) Y, \tag{8}$$

for all vector fields, X and Y.

Theorem

Let $\{e_1, e_2, \cdots, e_{n-k}\}$ be an orthogonal basis for D. The generalized Christoffel symbols of $\tilde{\nabla}$ are:

$$\tilde{\Gamma}^i_{jk} = \frac{1}{\|e_i\|^2} \langle\langle \nabla_{e_j} e_k, e_i \rangle\rangle, \tag{9}$$

and the equation of motion (Equation 7) becomes:

$$\dot{v}^i + \tilde{\Gamma}^i_{jk} v^j v^k = \sum_{a=1}^{m} Y^i_a u_a, \tag{10}$$

where v^i are the components of $\dot{q}$ along $\{e_1, e_2, \cdots, e_{n-k}\}$, i.e. $\dot{q} = v^i e_i$ and where the coefficient of control forces is:

$$Y_a^i = \frac{1}{\|e_i\|^2} \langle F_a, e_i \rangle . \tag{11}$$

Of course, if the control forces are exact differentials (i.e. $F_a = d\varphi_a$ for some $a \in \{1, \cdots, m\}$), then:

$$Y_a^i = \frac{1}{\|e_i\|^2} \mathsf{L}_{e_i} \varphi_a, \tag{12}$$

where $\mathsf{L}_{e_i}\varphi_a$ is the Lie derivative of scalar function φ_a, with respect to vector e_i (note that the Lie derivative of function f, with respect to vector X, is defined as:

$$\mathrm{L}_X f = \langle\langle \mathrm{grad}(f), X \rangle\rangle).$$

MODELING OF THE SNAKEBOARD VIA CONSTRAINED AFFINE CONNECTION

If one assumes that the rear and front platforms of the snakeboard have equal angles with opposite directions at each instant of time during motion (this is not far from the real situation, where riders of the snakeboard usually move their feet in equal but opposite directions) he/she has five dimensional configuration manifolds, i.e. $(x, y, \theta, \psi, \phi)$, to describe the position of the snakeboard, where x and y are the locations of the snakeboard's center of mass; θ is the angle of the bar relative to a fixed frame; ψ is the relative angle between the bar and the rotor, playing the role of the human torso and ϕ is the relative angle between the bar and the horizontal axes of the wheels, as shown in Figure 2.

One can write the Lagrangian for the snakeboard as:

$$L = \frac{1}{2} m(\dot{x}^2 + \dot{y}^2) + \frac{1}{2} J\dot{\theta}^2 + \frac{1}{2} J_r(\dot{\psi} + \dot{\theta})^2 + \frac{1}{2} J_w(\dot{\phi} + \dot{\theta})^2, \tag{13}$$

where J is the snakeboard body inertia, J_r is the rotor inertia and $\frac{1}{2}J_w$ is the inertia of each wheel all about the axis, which is perpendicular to the plane of the motion, and m is the mass of the system. So, one can write the metric tensor G as:

$$G = \begin{pmatrix} m & 0 & 0 & 0 & 0 \\ 0 & m & 0 & 0 & 0 \\ 0 & 0 & J + J_r + J_w & J_r & J_w \\ 0 & 0 & J_r & J_r & 0 \\ 0 & 0 & J_w & 0 & J_w \end{pmatrix}. \tag{14}$$

For no sideway slipping of the wheels, the constraints are:

$$-\sin(\theta - \phi)\dot{x} + \cos(\theta - \phi)\dot{y} + l\cos(\phi)\dot{\theta} = 0,$$
$$-\sin(\theta + \phi)\dot{x} + \cos(\theta + \phi)\dot{y} - l\cos(\phi)\dot{\theta} = 0. \tag{15}$$

In one-form format, these can be expressed as (see Equation 5):

$$\omega_1 = -\sin(\theta - \phi)dx + \cos(\theta - \phi)dy + l\cos(\phi)d\theta,$$
$$\omega_2 = -\sin(\theta + \phi)dx + \cos(\theta + \phi)dy - l\cos(\phi)d\theta. \tag{16}$$

Now, relative to the dimension of D, which is $n-k = 3$, one can introduce the following basis:

$$e_1' = l\cos\phi\left(\cos\theta\frac{\partial}{\partial x} + \sin\theta\frac{\partial}{\partial y}\right) - \sin\phi\frac{\partial}{\partial \theta},$$
$$e_2' = \frac{\partial}{\partial \psi},$$
$$e_3' = \frac{\partial}{\partial \phi}, \tag{17}$$

where e_1' corresponds to the instantaneous center of rotation when ψ and ϕ are fixed (see Figure 2) and $\{e_2', e_3'\}$ describe the changes in ψ and ϕ, respectively. To use the above vectors in Equation 9, they must be orthogonal. Since e_1' is orthogonal to e_3', an effort is made to find an appropriate form for e_2'.

Using the Gram Schmidt procedure, one can find an orthogonal basis as follows:

$$e_1 = e_1',$$
$$e_2 = e_2' - \frac{\langle\langle e_2', e_1\rangle\rangle}{\langle\langle e_1, e_1\rangle\rangle} e_1 = \alpha\left(\cos\theta\frac{\partial}{\partial x} + \sin\theta\frac{\partial}{\partial y}\right) - \beta\frac{\partial}{\partial \theta} + \frac{\partial}{\partial \psi},$$
$$e_3 = e_3', \tag{18}$$

where:

$$\alpha = \frac{J_r l \cos\phi\sin\phi}{\gamma}, \qquad \beta = \frac{J_r\sin^2\phi}{\gamma},$$
$$\gamma = ml^2\cos^2\phi + (J + J_r + J_w)\sin^2\phi. \tag{19}$$

In the presented model, the control forces are torques applied at the rotor and wheel axles. In one-form forms, they can be represented by $F_\psi = d\psi$ and $F_\phi = d\phi$. By using Equations 11, one has:

$$Y_\psi = \frac{\gamma}{J_r\delta} e_2, \qquad Y_\phi = \frac{1}{J_w} e_3, \tag{20}$$

where:

$$\delta = ml^2\cos^2\phi + (J + J_w)\sin^2\phi. \tag{21}$$

All generalized Christoffel symbols defined in Equation 9 vanish, except the following:

$$\tilde{\Gamma}^1_{13} = \frac{(J + J_r + J_w - ml^2)\cos\phi\sin\phi}{\gamma},$$

$$\tilde{\Gamma}^1_{23} = \frac{J_r ml^2\cos\phi}{\gamma^2}, \qquad \tilde{\Gamma}^2_{13} = -\frac{2ml^2\cos\phi}{\delta},$$

$$\tilde{\Gamma}^2_{23} = -\frac{J_r ml^2\cos\phi\sin\phi}{\gamma\delta}. \tag{22}$$

Now, one can write the dynamic equation of the snakeboard by using Equation 10:

$$\dot{v} + \tilde{\Gamma}^1_{13} v\dot{\phi} + \tilde{\Gamma}^1_{23}\dot{\psi}\dot{\phi} = 0,$$

$$\ddot{\psi} + \tilde{\Gamma}^2_{13} v\dot{\phi} + \tilde{\Gamma}^2_{23}\dot{\psi}\dot{\phi} = \frac{\gamma}{J_r\delta}u_\psi,$$

$$\ddot{\phi} = \frac{1}{J_w}u_\phi. \tag{23}$$

Note that $\dot{\psi}$ and $\dot{\phi}$ are written for the velocity component along e_2 and e_3, respectively. Next, the kinematic equations of motion are written, i.e. $\dot{q} = ve_1 + \dot{\psi}e_2 + \dot{\phi}e_3$, as:

$$\begin{pmatrix}\dot{x}\\ \dot{y}\\ \dot{\theta}\end{pmatrix} = \begin{pmatrix} l\cos\phi\cos\theta \\ l\cos\phi\sin\theta \\ -\sin\phi\end{pmatrix} v + \begin{pmatrix}\alpha\cos\theta \\ \alpha\sin\theta \\ -\beta\end{pmatrix}\dot{\psi}. \tag{24}$$

In what follows, Equations 23 and 24 are used to find some new gaits for the snakeboard.

EXAMPLES

Three famous gaits of the snakeboard are forward, rotation and parallel parking (see [1] for details), which were developed especially to explain controllability ideas rather than nonlinear behaviors of the snakeboard. In this study of snakeboard locomotion, it is endeavored to find some robust gaits in forward and rotation gaits (the famous forward gait developed in [1] is not stable and the rotation gait is not repetitive) and also some gaits based on stable limit cycles.

In the examples, ψ and ϕ are assumed to be simple harmonic functions of time;

$$\psi = a_\psi \sin(\omega_\psi t + \varphi_\psi),$$

$$\phi = a_\phi \sin(\omega_\phi t + \varphi_\phi), \tag{25}$$

where a, ω and φ are amplitude, frequency and phase, respectively. All numerical values for snakeboard geometry, such as l, m, J etc., are taken from [1] and the initial conditions for the described examples are assumed to be $(x, y, \theta) = (0, 0, 0)$ and $(\varphi_\psi, \varphi_\phi) = (\pi, 0)$.

k_o and k_a are defined as the ratio of frequencies and amplitudes of ϕ to ψ, respectively. The gaits of the examples are produced for different values of k_o and k_a, fixing $a = a_\psi$ and $\omega = \omega_\psi$ in each case.

Case 1 (Some Pseudo Forward Gaits)

Assume that $a = \frac{\pi}{4}$, $\omega = 1$ and $k_o = \frac{m}{n}$. If $m = 1$ and n is an odd number, one has unstable gaits (see also [3,5]), which are forward for $n = 1$ (the famous forward gait) and $n = 3$ (see Figure 3). Here, some pseudo forward but stable gaits are developed for $k_o = \frac{3}{5}$ (fishbone-like gait) and $k_o = \frac{3}{4}$ (moving limit cycle gait). These gaits are named pseudo-forward, because their net forward displacement is produced by moving cycles. Also, they deviate negligibly from the positive x axis. These gaits are drawn for different values of k_a (see Figures 4 and 5). Although, in the "fishbone-like" gait, the qualitative behavior does not change with different values of k_a, in the "moving limit cycle gait", these behaviors converge to a stable limit cycle (see Figure 5).

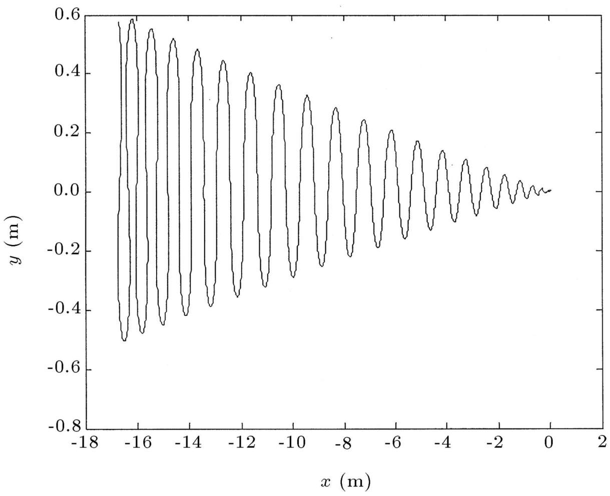

Figure 3a. Unstable forward gait $(a, k_o, k_a) = (\pi/4, 1/3, 1)$ after 400 seconds.

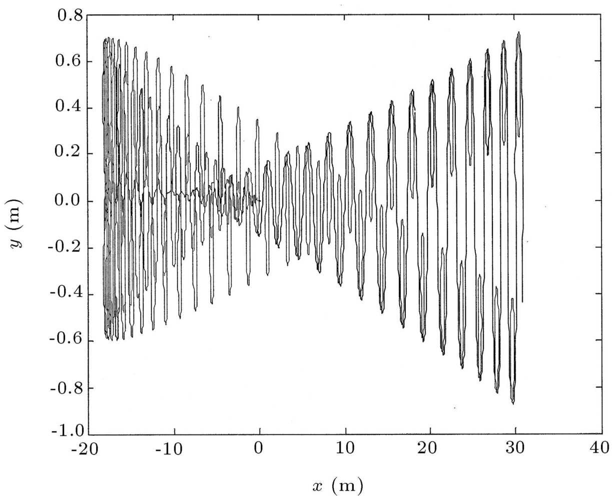

Figure 3b. Unstable forward gait $(a, k_o, k_a) = (\pi/4, 1/3, 1)$ after 1000 seconds.

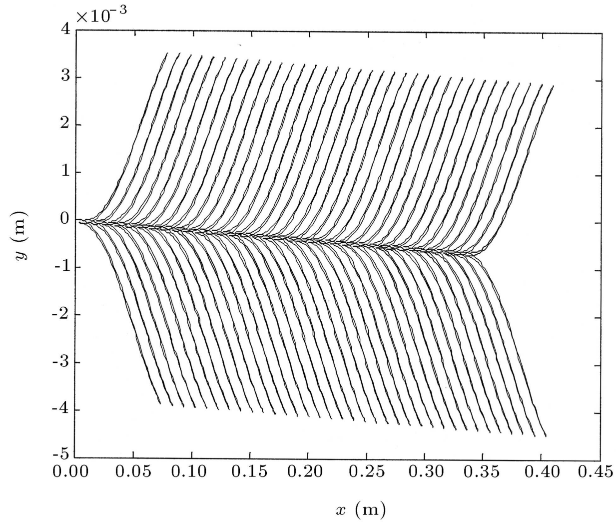

Figure 4a. Fishbone-like gait $(a,\, k_o,\, k_a) = (\pi/4,\, 3/5,\, 1/2)$.

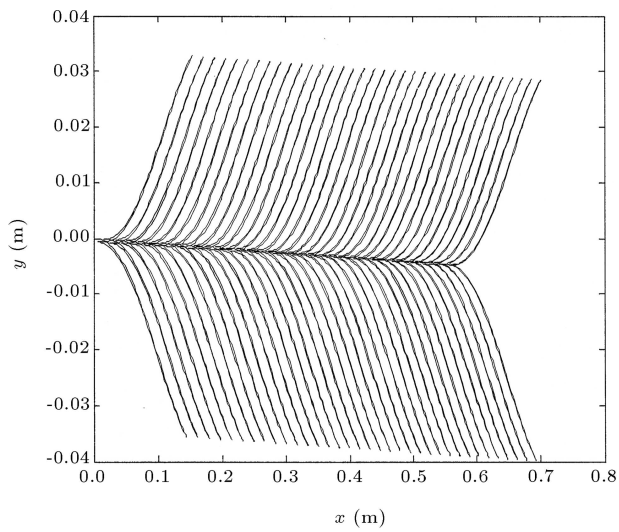

Figure 4b. Fishbone-like gait $(a,\, k_o,\, k_a) = (\pi/4,\, 3/5,\, 1)$.

Case 2 (Some Robust Rotation and Stable Limit Cycle Gaits)

For k_o equal to $\frac{1}{4}$, $\frac{2}{4}$ and/or $\frac{3}{4}$, some gaits, which are repetitive and robust, are developed. The robust rotation and stable limit cycle gaits with different values of k_a are shown in Figures 5d, 6 and 7. All the above gaits can also be produced with a real snakeboard (because $a = \frac{\pi}{4}$ is an acceptable amplitude in real situations). Besides, some limit cycles are developed that can be produced only by experimental modeling of the snakeboard, i.e., their assumed amplitudes cannot be normally produced by humans. These latter gaits have the same k_o as the former ones, but their amplitude, i.e. $a = a_\psi$, are equal to π, $\frac{3\pi}{4}$ or $\frac{2\pi}{3}$ (see Figures 8 to 10 for details).

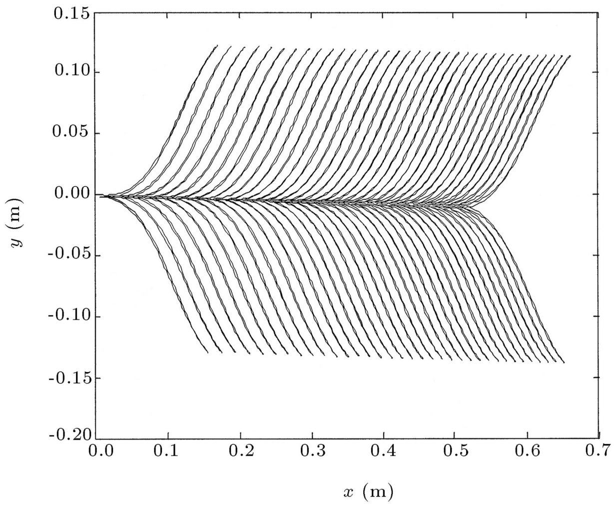

Figure 4c. Fishbone-like gait $(a,\, k_o,\, k_a) = (\pi/4,\, 3/5,\, 1.5)$.

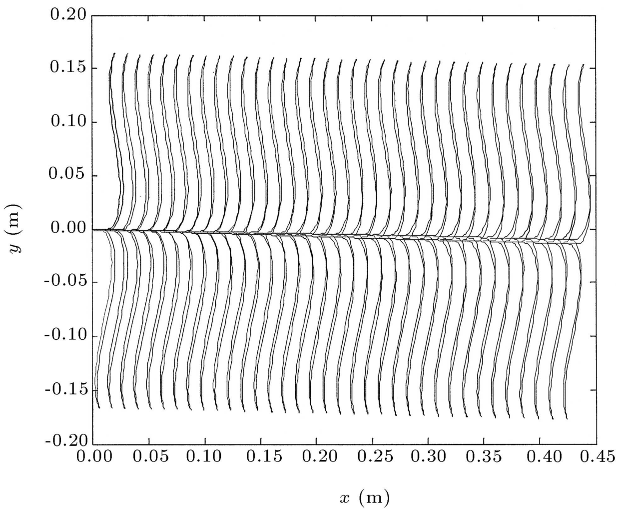

Figure 4d. Fishbone-like gait $(a,\, k_o,\, k_a) = (\pi/4,\, 3/5,\, 2)$.

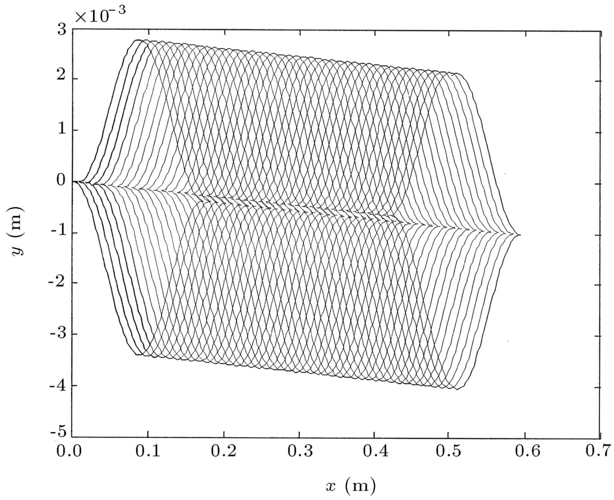

Figure 5a. Moving limit cycle gait $(a,\, k_o,\, k_a) = (\pi/4,\, 3/4,\, 1/2)$.

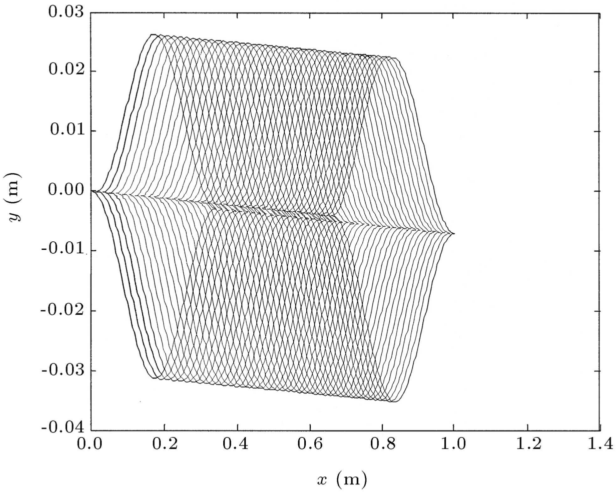

Figure 5b. Moving limit cycle gait $(a, k_o, k_a) = (\pi/4, 3/4, 1)$.

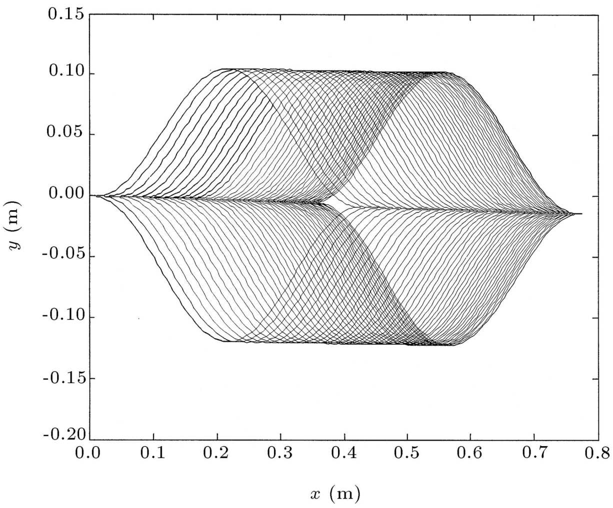

Figure 5c. Moving limit cycle gait $(a, k_o, k_a) = (\pi/4, 3/4, 1.5)$.

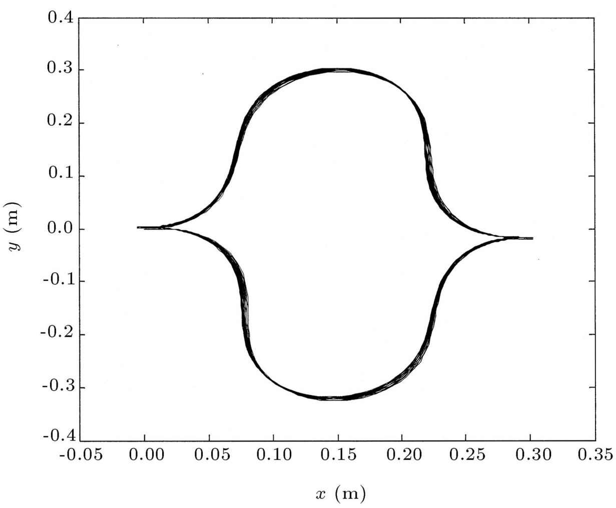

Figure 5d. Limit cycle gait $(a, k_o, k_a) = (\pi/4, 3/4, 1.75)$.

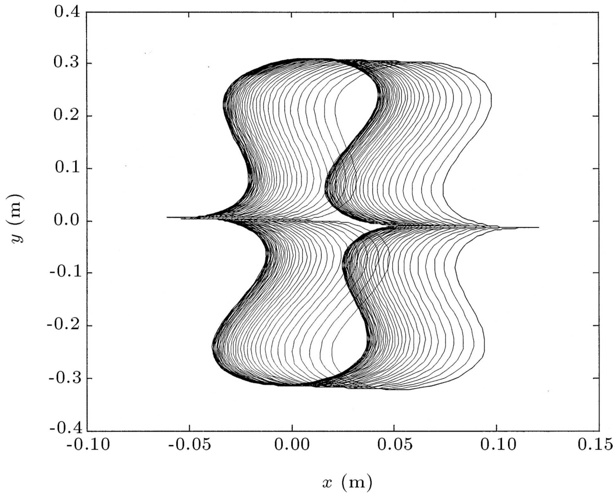

Figure 5e. Moving limit cycle gait $(a, k_o, k_a) = (\pi/4, 3/4, 1.9)$.

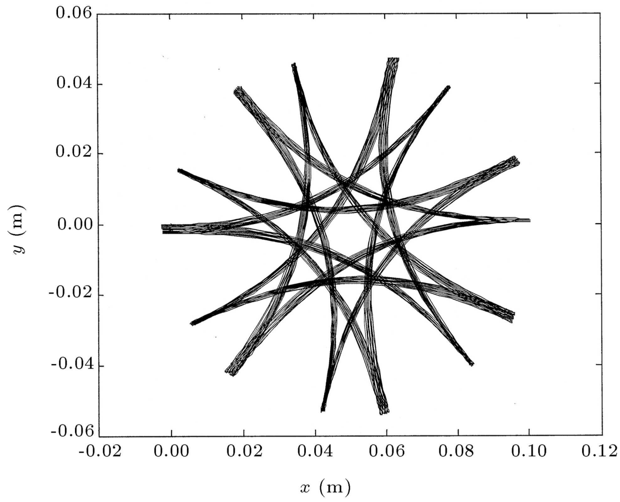

Figure 6. Robust rotation gait $(a, k_o, k_a) = (\pi/4, 1/2, 1.15)$.

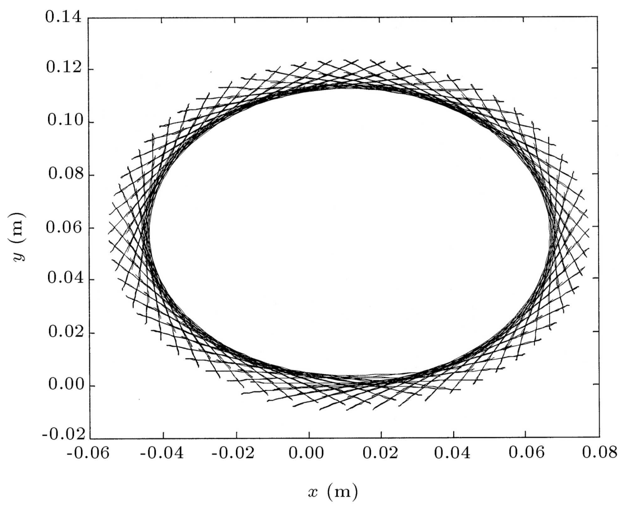

Figure 7. Limit cycle gait $(a, k_o, k_a) = (\pi/4, 1/4, 1)$.

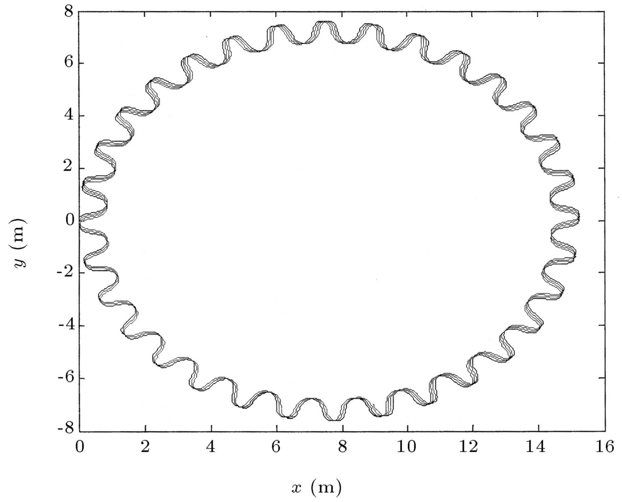

Figure 8. Limit cycle gait (a, k_o, k_a) = ($2\pi/3$, 1/4, 1.75).

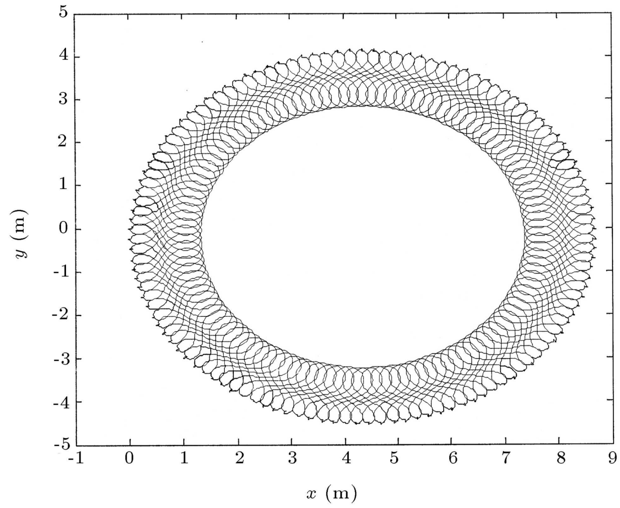

Figure 9. Limit cycle gait (a, k_o, k_a) = (π, 1/4, 1.2).

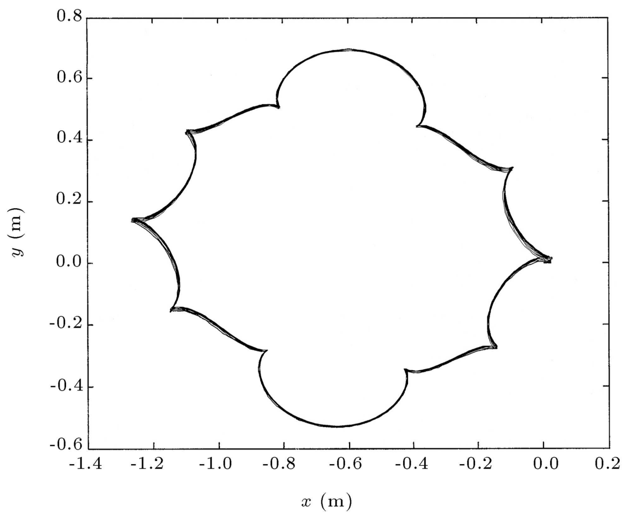

Figure 10. Limit cycle gait (a, k_o, k_a) = ($3\pi/4$, 3/4, 1.075).

CONCLUSION

It was shown that a snakeboard, as the prototype of a nonholonomic locomotion system with symmetry, is capable of generating highly coherent robust gaits. Some of these gaits were produced through proper adjustment of the input parameters. The essential features of the mathematical model, namely, nonlinearity and symmetry, may be regarded as the source of complexity and coherency of these gaits. Although these patterns were generated by an ad hoc tuning of certain parameters, further study may reveal corroborative evidence in favor of a causal relation between tuning criteria and complex coherent patterns.

NOMENCLATURE

∇	affine connection
Γ^i_{jk}	Christoffel symbols
$\varphi_\psi, \varphi_\phi$	snakeboard's phases of the shape variables
λ	Lagrange multipliers
ψ, ϕ	snakeboard's body coordinates
ω^i_j	constraint one-forms
$\omega, \omega_\psi, \omega_\phi$	snakeboard's frequencies of the shape variables
a, a_ψ, a_ϕ	snakeboard's amplitudes of the shape variables
D	constraint distribution
F_i	generalized forces
G	kinetic energy metric tensor
J, J_r, J_w	snakeboard's body, rotor and wheel inertias
k_o, k_a	the ratio of frequencies and amplitudes of ϕ to ψ, respectively
L	Lagrangian
L	Lie derivative operator
m	mass of the snakeboard
q^i	generalized coordinates
Q	configuration manifold
TQ	tangent space of Q
x, y, θ	snakeboard's center of mass position

REFERENCES

1. Lewis, A.D., Ostrowski, J.P., Burdick, J.W. and Murray, R. "Nonholonomic mechanics and locomotion: The snakeboard example", *Proceedings of the 1994 IEEE International Conference on Robotics and Automation*, San Diego, CA, USA, pp 2391-2400 (1994).

2. Kelly, S.D. and Murray, R.M. "Geometric phases and locomotion", *J. Robotic Systems*, **12**(6), pp 417-431, (1995).

3. Ostrowski, J.P. and Burdick, J.W. "The geometric mechanics of undulatory robotic locomotion", *International Journal of Robotics Research*, **17**(7), pp 683-701 (1998).

4. Lewis, A.D. "Simple mechanical control systems with constraints", *IEEE TAC*, **45**(8), pp 1420-1436 (2000).

5. Ostrowski, J.P. "The mechanics and control of undulatory robotic locomotion", PhD thesis, California Institute of Technology, Pasadena, CA, USA (1995).

6. Ostrowski, J. and Burdick, J. "Controllability tests for mechanical systems with constraints and symmetries", *J. of Applied Mathematics and Computer Science*, **7**(2), pp 101-127 (1997).

7. Bullo, F., Leonard, N.E. and Lewis, A.D. "Controllability and motion algorithms for underactuated Lagrangian systems on Lie groups", *IEEE TAC*, **45**(8), pp 1437-1454 (2000).

8. Bullo, F., Lewis, A.D. and Lynch, K.M. "Controllable kinematic reductions for mechanical systems: Concepts, computational tools, and examples", *2002 Int. Symp. on Mathematical Theory of Networks and Systems (MTNS 2002)*, Notre Dame, IL, USA (2002).

9. Ostrowski, J.P. "Steering for a class of dynamic nonholonomic systems", *IEEE Trans. on Automatic Control*, **45**(8), pp 1492-1497 (2000).

10. Murray, R.M. and Sastry, S.S. "Nonholonomic motion planning: Steering using sinusoids", *IEEE Transactions on Automatic Control*, **38**(5), pp 700-716 (1993).

11. Ostrowski, J., Desai, J.P. and Kumar, V. "Optimal gait selection for nonholonomic locomotion systems", *Int. J. of Robotics Research*, **19**(3), pp 225-237 (2000).

12. Bullo, F. and Lynch, K.M. "Kinematic controllability for decoupled trajectory planning in underactuated mechanical systems", *IEEE Trans. on Robotics and Automation*, **17**(4), pp 402-412 (2001).

13. Bullo, F. and Lewis, A.D. "Kinematic controllability and motion planning for the snakeboard", *IEEE TRA*, **19**(3), pp 494-498 (2002).

14. Iannitti, S. and Lynch, K.M. "Exact minimum control switch motion planning for the snakeboard", *IEEE/RSJ International Conference on Intelligent Robots and Systems*, Las Vegas, NV (2003).

15. Iannitti, S. and Lynch, K.M. "Minimum control switch motions for the snakeboard: A case study in kinematically controllable underactuated systems", *IEEE Transactions on Robotics*, **20**(6), pp 994-1006 (2004).

16. Shammas, S. "Generalized motion planning for underactuated mechanical systems", Ph.D. Thesis, Carnegie Mellon University, Pittsburgh, Pennsylvania (2006).

17. Abraham, R. and Marsden, J.E., *Manifold, Tensor Analysis and Applications*, Springer-Verlag, New York, (1988).

18. Bloch, A.M., Krishnaprasad, P.S., Marsden, J.E. and Murray, R.M. "Nonholonomic mechanical systems with symmetry", *Archive for Rational Mechanics and Analysis*, **136**(1), pp 21-99 (1996).

19. Marsden, J.E. and Ratiu, T.S., *Introduction to Mechanics and Symmetry*, Springer-Verlag, 2nd Edition, New York, USA (1999).

20. Bullo, F. and Zefran, M. "On mechanical control systems with nonholonomic constraints and symmetries", *System & Control Letters*, **45**(2), pp 133-143 (2002).